

Analysis of Transients in a 4-Level Flying Capacitor Converter: Time Domain Approach. Part 1: Large Normalised Voltage Command

Research Article

Boris Reznikov¹, Alex Ruderman², Valentina Galanina³

¹GS Group, St. Petersburg, Russia

²Department of Electrical and Computer Engineering, Nazarbayev University, Nur-Sultan, Kazakhstan, Israel

³Department of Applied Mathematics, State University of Aerospace Instrumentation, St. Petersburg, Russia

Received October 03, 2019; Accepted January 05, 2020

Abstract: A 4-level flying capacitor converter (FCC) operation is considered on a base of discrete state-space model. A transition matrix is obtained for a pulse width modulation (PWM) period for large normalised voltage command values [1/3, 1). The transition matrix elements are expanded into power series by small parameters. The matrix eigenvalues are presented in the form of power series as well. Six separate transients are constructed for six possible initial FCC states on a PWM period. Inductor current and capacitors' voltage transients are found for the voltage source power-up as the arithmetic average of the six separate transients. Finally, the discrete solutions are replaced by equivalent continuous ones. Simple and accurate formulas for inductor current and capacitors' voltage transients demonstrate good agreement with simulation results.

Keywords: 4-level DC–DC converter • flying capacitor • natural balancing • transients

1. Introduction

Time domain approach for average transients in a three-level DC–DC flying capacitor converter (FCC) was first described in detail in Reznikov et al. (2019). In that paper, the processes in “short” and “long” time were separated and the strict and detailed analysis was carried out for “long” time process. The paper introduced the definitions of partial and averaged transients and presented simple and accurate formulas for the transients of three-level FCC. In comparison with the three-level FCC, a four-level one potentially has smaller ripples for steady-state load current and capacitor voltages due to the higher number of output voltage levels. It was previously noted (Reznikov et al., 2019) that the frequency domain approach (Wilkinson et al., 2006a, 2006b; Yang et al., 2001) leads to extremely cumbersome formulas that do not allow to trace the dependence of the transient characteristics on the FCC circuit, load and pulse width modulation (PWM) parameters. The time domain approach to natural balancing dynamics of a four-level FCC was first presented in Reznikov and Ruderman (2009). Owing to the conference paper size limitation, some main ideas were formulated briefly and declaratively. Partial transients for capacitors voltages (formulas (25) and (26) in Reznikov and Ruderman, 2009) are obtained using a simplified technique (Ruderman and Reznikov, 2010) without giving important details. The accurate load current average dynamics are not presented. In addition, there is no strict derivation of the average steady-state capacitor voltages. It should be noted that the resulting transients correspond to only one sequence of FCC switching topologies on a PWM period.

The purpose of this paper was to present a strict and detailed derivation of simple and accurate formulas for average transients that clearly show the dependences of the FCC circuit and PWM period parameters on the basis of ideas presented in Reznikov et al. (2019) for a three-level FCC.

* Email: b_reznikov@mail.ru

2. The Problem Formulation. Discrete Model

Figure 1a shows a four-level DC–DC FCC topology. The transient analysis is carried out under the assumptions accepted for a three-level FCC (Reznikov et al., 2019), namely, the load is represented as a series connection of inductance and resistor, the switches are bi-directional with zero resistance in the conductive state (ON) and infinite in the open-circuit one (OFF) and switching times are negligibly small.

Owing to the FCC symmetry, its operation will be analysed only for positive normalised voltage command D . For the four-level FCC carrier-based PWM (Reznikov and Ruderman, 2009), the switching sequences of complementary switch pairs $S1-\bar{S}1$, $S2-\bar{S}2$ and $S3-\bar{S}3$ differ for the two ranges of D , which are separated by $D = 1/3$. Therefore, the FCC operation is considered for large D , namely $1/3 \leq D < 1$, and small D , that is $0 \leq D \leq 1/3$. This paper (Part 1) addresses FCC operation for large D .

The carrier-based PWM is discussed in detail in Reznikov and Ruderman (2009). A PWM period T_{PWM} is divided into six successive time intervals $\Delta t_1, \Delta t_2, \Delta t_3, \Delta t_4, \Delta t_5, \Delta t_6$, each with its own equivalent circuit (with the number equal to the index of respective time interval). The time intervals with even (odd) indices have the same duration $\Delta t_2 = \Delta t_4 = \Delta t_6$ ($\Delta t_1 = \Delta t_3 = \Delta t_5$).

Figure 1b shows FCC topologies for large D . Time intervals with even indices correspond to the same topology, so there are only four different types of topologies. The topologies are defined by the following switches states. In Topology 1, switches $S3$ and $S2$ are ON, and switch $S1$ is OFF. In Topology 3, switches $S1$ and $S3$ are ON, and switch $S2$ is OFF. In Topology 5, switches $S1$ and $S2$ are ON, and switch $S3$ is OFF. For Topologies 2, 4 and 6, all three switches $S1$, $S2$ and $S3$ are ON.

Any topology of Figure 1b is a linear circuit of either first or second order. This means that, given the values of inductance current i_L and capacitor voltages of v_{C1} and v_{C2} at the beginning of time interval t_k , one can obtain their values at the end of this interval by solving the corresponding linear differential equations. Let the state-space vector for the four-level FCC be $X(t) = (i_L(t) \ v_{C1}(t) \ v_{C2}(t))^T$. Then, the matrix relation for time interval Δt_k may be written as

$$X(t + \Delta t_k) = A_k(\Delta t_k)X(t) + B_k(\Delta t_k)\frac{V}{2} \tag{1}$$

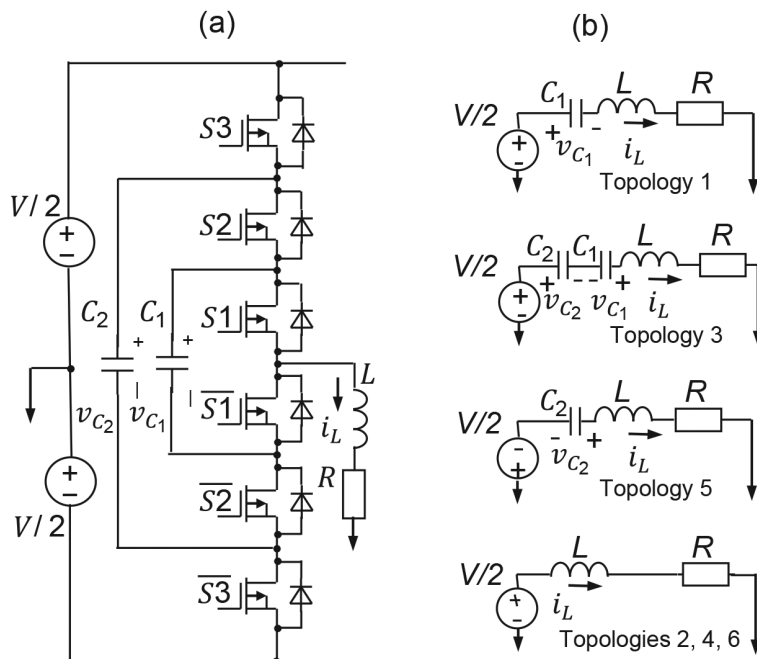


Fig. 1. Four-level FCC circuit (a) and its switched topologies (b). Large D case.

where matrices A_k and vectors B_k are defined by topologies and durations of the respective time intervals. For the sake of simplicity, A_k and B_k arguments from now on will be omitted.

Writing down equation (1) subsequently for each of six PWM period T_{PWM} intervals and accounting for the continuity of the state-space coordinates at the switching moments yield

$$X^{(1)}(t+T_{PWM}) = A^{(1)}X^{(1)}(t) + B^{(1)}V/2 \quad (2)$$

where transient matrix $A^{(1)}$ and vector $B^{(1)}$ are defined as

$$A^{(1)} = A_6 A_5 A_4 A_3 A_2 A_1 \quad (3)$$

$$B^{(1)} = A_6 \left(A_5 \left(A_4 \left(A_3 \left(A_2 B_1 + B_2 \right) + B_3 \right) + B_4 + B_5 \right) + B_6 \right) \quad (4)$$

Equations similar to equation (2) can be obtained starting from any interval from the second to sixth. Then, the matrix and vector will be different from those of equations (3) and (4) by a cyclic permutation of indices of matrices A_k and vectors B_k . To establish a correspondence between the matrix and vector in equation (2) and the number of the initial interval, the superscript in parentheses equals to the number of the initial interval. A detailed analysis below assumes that the PWM period starts with the time interval 1.

The use of equation (2) (the discrete model of the FCC) assumes giving up the details of FCC behaviour within a PWM period. Using the terminology (Reznikov et al., 2019), the FCC behaviour in the “short” time is ignored, and the focus is put on the average behaviour in the “long” time by considering the FCC behaviour at the discrete moments t_k . In accordance with the above, let us rewrite equation (2) as

$$X^{(1)}(t_{k+1}) = A^{(1)}X^{(1)}(t_k) + B^{(1)}\frac{V}{2}, \quad t_{k+1} = t_k + T_{PWM} \quad (5)$$

As shown in Reznikov and Ruderman (2009), the durations of the time intervals for large D become

$$\Delta t_1 = \Delta t_3 = \Delta t_5 = \frac{1-|D|}{2}T_{PWM} \quad (6)$$

$$\Delta t_2 = \Delta t_4 = \Delta t_6 = \frac{|D|-1/3}{2}T_{PWM} \quad (7)$$

As matrices A_i and vectors B_i elements are the solutions of linear differential equations, they are expressed by functions $\cos\omega\tau$, $\sin\omega\tau$ and $\exp(-\alpha\tau)$. For different topologies, ω equals to one of three values: $\omega_1 = \sqrt{(1/LC_1) - \alpha^2}$, $\omega_2 = \sqrt{(1/LC_2) - \alpha^2}$, $\omega_3 = \sqrt{((C_2 + C_1)/LC_2C_1) - \alpha^2}$ and $\alpha = R/(2L)$. Let us use a small parameter introduced similar to Reznikov et al. (2019). Since during time intervals $\Delta t_1, \dots, \Delta t_6$ the state-space coordinates do not change much, any value $\omega_1\Delta t_i$, $\omega_2\Delta t_i$, $\omega_3\Delta t_i$, $\alpha\Delta t_i$ is small. It is convenient to choose as a small parameter the value $\beta = \omega_1((1-|D|)/2)T_{PWM}$. As only positive D is considered, in the following, D is used instead of its absolute value. Let us use the following designations: $s_-(\omega) = \cos\omega\tau - (\alpha/\omega)\sin\omega\tau$, $s_+(\omega) = \cos\omega\tau + (\alpha/\omega)\sin\omega\tau$ and $r_c = C_1/C_2$. After simple transformations, $\omega_2 = k_1\omega_1$ and $\omega_3 = k_2\omega_1$, where $k_1 = \sqrt{r_c(1+r^2) - r^2}$ and $k_2 = \sqrt{r_c(1+r^2) + 1}$. Denote also $w_-(k) = \cos k\beta - (r/k)\sin k\beta$ and $w_+(k) = \cos k\beta + (r/k)\sin k\beta$. The above designations allow representing matrices A_k and vectors B_k in a compact form as functions of β .

$$A_1 = e^{-r\beta} \begin{pmatrix} w_-(1) & -\frac{\sin\beta}{\omega_1 L} & 0 \\ \omega_1 L(1+r^2)\sin\beta & w_+(1) & 0 \\ 0 & 0 & e^{r\beta} \end{pmatrix}$$

$$A_3 = e^{-r\beta} \begin{pmatrix} w_-(k_1) & \frac{\sin k_1 \beta}{k_1 \omega_1 L} & -\frac{\sin k_1 \beta}{k_1 \omega_1 L} \\ -\frac{\omega_1}{k_1} L(1+r^2) \sin k_1 \beta & \frac{w_1(k_1) + r_c e^{r\beta}}{1+r_c} & r_c \frac{w_1(k_1) + e^{r\beta}}{1+r_c} \\ \frac{\omega_1 r_c}{k_1} L(1+r^2) \sin k_1 \beta & \frac{w_1(k_1) + e^{r\beta}}{1+r_c} & \frac{r_c w_1(k_1) + e^{r\beta}}{1+r_c} \end{pmatrix}$$

$$A_5 = e^{-r\beta} \begin{pmatrix} w_-(k_2) & 0 & \frac{\sin k_2 \beta}{k_2 \omega_1 L} \\ 0 & e^{r\beta} & 0 \\ -\frac{\omega_1 r_c}{k_2} L(1+r^2) \sin k_2 \beta & 0 & w_+(k_2) \end{pmatrix}$$

$$A_2 = \begin{pmatrix} e^{-2r\beta \frac{d-1/3}{1-d}} & 0 & 0 \\ 0 & 1 & 0 \\ 0 & 0 & 1 \end{pmatrix}$$

$$A_2 = A_4 = A_6$$

$$B_1 = \begin{pmatrix} \frac{\exp(-r\beta) \sin \beta}{\omega L} \\ 1 - \exp(-r\beta) (\cos \beta + r \sin \beta) \\ 0 \end{pmatrix} \quad B_3 = \begin{pmatrix} \frac{\exp(-r\beta) \sin(\beta k_1)}{\omega L k_1} \\ \frac{\exp(-r\beta) \left(\cos(\beta k_1) + \frac{r}{k_1} \sin(\beta k_1) \right) - 1}{1+r_c} \\ \frac{1 - \exp(-r\beta) \left(\cos(\beta k_1) + \frac{r}{k_1} \sin(\beta k_1) \right)}{1+r_c} r_c \end{pmatrix}$$

$$B_5 = \begin{pmatrix} -\frac{\exp(-r\beta) \sin(\beta k_2)}{\omega L k_2} \\ 0 \\ 1 - \exp(-r\beta) \left(\cos(\beta k_2) + \frac{r}{k_2} \sin(\beta k_2) \right) \end{pmatrix} \quad B_2 = B_4 = B_6 = \begin{pmatrix} \frac{1 - \exp\left(-2r\beta \frac{D-1/3}{1-D}\right)}{R} \\ 0 \\ 0 \end{pmatrix}$$

3. Eigenvalues

Let us expand the matrix A_i elements into series of β and multiply the matrices according to equation (3). The elements of the matrix product (3) are also presented in the form of series of β :

$$A^{(1)} = \left\{ a_{ij}^{(1)} \right\}_{i=1}^3 \quad (8)$$

$$a_{11}^{(1)} = 1 - \frac{4r\beta}{1-D} + \frac{8r^2\beta^2}{(1-D)^2} + \frac{2\left(\left(1+r^2\right)\left(1+D\right)\left(-1+d\right)^2\left(1+r_c\right)-16r^2\right)\beta^3}{3(1-D)^3} + \dots \quad (9)$$

$$a_{12}^{(1)} = \frac{4r\beta^2}{3\omega L(1-D)} - \frac{(3r_c(1+r^2)(1-D)^2 + 8r^2(3D+7))\beta^3}{18\omega L(1-D)^2} + \dots \quad (10)$$

$$a_{13}^{(1)} = \frac{4r\beta^2}{3\omega L(1-D)} + \frac{((1-D)^2 + r^2(D^2 - 10D - 7))\beta^3}{6\omega L(1-D)^2} + \dots \quad (11)$$

$$a_{21}^{(1)} = \frac{4\omega Lr(1+r^2)\beta^2}{3(1-D)} + \frac{\omega L(1+r^2)(3r_c(1+r^2)(1-D)^2 + 8r^2(3D-5))\beta^3}{18(1-D)^2} + \dots \quad (12)$$

$$a_{22}^{(1)} = 1 - \frac{2r(1+r^2)(1+D)\beta^3}{3(1-D)} + \dots \quad (13)$$

$$a_{23}^{(1)} = \frac{(1+r^2)\beta^2}{2} - \frac{r(1+r^2)\beta^3}{3} + \dots \quad (14)$$

$$a_{31}^{(1)} = \frac{4\omega Lr_c r(1+r^2)\beta^2}{3(1-D)} - \frac{\omega Lr_c(1+r^2)(r^2(D-5)^2 + (1-D)^2)\beta^3}{6(1-D)^2} + \dots \quad (15)$$

$$a_{32}^{(1)} = -\frac{r_c(1+r^2)\beta^2}{2} - \frac{r_c r(1+r^2)\beta^3}{3} + \dots \quad (16)$$

$$a_{33}^{(1)} = 1 - \frac{2r_c r(1+r^2)(1+D)\beta^3}{3(1-D)} + \dots \quad (17)$$

The matrix $A^{(1)}$ eigenvalues are the roots of characteristic polynomial $p(\lambda) = \det(A^{(1)} - \lambda E)$, where E is a unity 3×3 matrix. All other transient matrices $A^{(i)}$, $i = 2, 3, 4, 5, 6$, will have the same eigenvalues, as they differ the matrix factors' cyclic permutation. Calculation of the polynomial coefficients through the matrix elements and their expansion in a series of β leads to

$$p(\lambda) = \lambda^3 + g_1\lambda^2 + g_2\lambda + g_3 \quad (18)$$

where

$$g_1 = -3 + \frac{4r\beta}{1-D} - \frac{8r^2\beta^2}{(1-D)^2} + \frac{32r^3\beta^3}{3(1-D)^3} + \frac{(F_1r^4 + F_2r^2 + 9r_c(1-D)^4)\beta^4}{36(1-D)^4} + \dots \quad (19)$$

$$g_2 = 3 - \frac{8r\beta}{1-D} + \frac{16r^2\beta^2}{(1-D)^2} - \frac{64r^3\beta^3}{3(1-D)^3} - \frac{((F_1 - 384)r^4 + F_2r^2 + 9r_c(1-D)^4)\beta^4}{36(1-D)^4} + \dots \quad (20)$$

$$g_3 = -1 + \frac{4r\beta}{1-D} - \frac{8r^2\beta^2}{(1-D)^2} + \frac{32r^3\beta^3}{3(1-D)^3} - \frac{32r^4\beta^4}{3(1-D)^4} + \dots \quad (21)$$

with

$$F_1 = (9D^2 + 78D + 41)(1-D)^2 r_c + 32(3D^3 - 5D^2 + D - 11)$$

$$F_2 = 2(1-D)^2 \left((9D^2 + 30D + 25)r_c + 16(3D+1) \right)$$

In Reznikov and Ruderman (2009), the polynomial roots are calculated by Cardano formulas that are quite cumbersome. In this paper, using the method described in Reznikov et al. (2019), the roots are sought in the form of a series in β :

$$\lambda_i = u_0^{(i)} + u_1^{(i)}\beta + u_2^{(i)}\beta^2 + u_3^{(i)}\beta^3 + \dots \quad (22)$$

The superscript i defines the root number and, in the case of a third-order polynomial, takes the values 1, 2 and 3. Just as for the second-order polynomial Reznikov et al. (2019), the convergence of the series (22) is proved easily. Since the polynomial coefficients are represented by convergent series and Cardano formulas provide arithmetic operations with them, as well as raise to the power of 1/2 and 1/3, the series (22) converges.

Substitute equation (22) into equation (18) and equate the series to zero:

$$p(\lambda_i) = c_0^{(i)} + c_1^{(i)}\beta + c_2^{(i)}\beta^2 + c_3^{(i)}\beta^3 + c_4^{(i)}\beta^4 + \dots = 0 \quad (23)$$

Next, starting from lower powers, equate to zero the coefficients $c_j^{(i)}$ and find consistently the roots expansion series coefficients. For $c_0^{(i)}$ the equation is $c_0^{(i)} = (u_0^{(i)} - 1)^3 = 0$. Hence, for any i , that is for all roots, $u_0^{(i)} = 1$. Then, substituting the $u_0^{(i)}$ value into equation (22), $c_1^{(i)} = 0$, $c_2^{(i)} = 0$ and $c_3^{(i)} = u_1^{(i)^2}((D-1)u_1^{(i)} - 4r)/(D-1) = 0$. First, consider $u_1^{(1)} = 4r/(D-1)$. After using the same operations, $u_2^{(1)} = 8r^2/(1-D)^2$ and $u_3^{(1)} = (2r(-48r^2 + (1+r^2)(3D+1)(1-D)^2(1+r_c)))/(9(1-D)^3)$, which yields the first root series representation as

$$\lambda_1 = 1 - \frac{4r\beta}{1-D} + \frac{8r^2\beta^2}{(1-D)^2} + \frac{2r\left(\left(1+r^2\right)\left(3D+1\right)\left(1-D\right)^2\left(1+r_c\right) - 48r^2\right)\beta^3}{9(1-D)^3} + O(\beta^4) \quad (24)$$

To obtain the second root, consider the second value of $u_1^{(i)}$ for which $c_3^{(i)} = 0$, namely, $u_1^{(2)} = 0$. Then $u_2^{(2)} = -(j(1+r^2)/2)\sqrt{r_c}$ and $u_3^{(2)} = -((3D+1)r(1+r^2)(1+r_c))/(9(1-D))$. As the polynomial coefficients are real and the second root is complex, the third root is a complex conjugate to the second one and there is no need to seek it on separate. Thus, the second and the third roots are represented as

$$\lambda_{2,3} = 1 \mp j \frac{\left(1+r^2\right)r_c\beta^2}{2} - \frac{r\left(1+r^2\right)\left(3D+1\right)\left(1+r_c\right)\beta^3}{9(1-D)} + O(\beta^4) \quad (25)$$

Represent the complex conjugate roots λ_2 and λ_3 in an exponential form:

$$\lambda_2 = M \exp(j\varphi), \quad \lambda_3 = M \exp(-j\varphi), \quad (26)$$

where the module M and argument φ are defined as follows:

$$M = \sqrt{\text{Re}^2(\lambda_2) + \text{Im}^2(\lambda_2)} = 1 - \frac{r(1+r^2)(1+r_c)(3D+1)}{9(1-D)}\beta^3 + O(\beta^4) \quad (27)$$

$$\varphi = \left| \arctg \left(\frac{\text{Im}(\lambda_2)}{\text{Re}(\lambda_2)} \right) \right| = \frac{(1+r^2)\sqrt{r_c}}{2}\beta^2 + O(\beta^4) \quad (28)$$

From equation (27), we can observe that the module of the roots λ_2 and λ_3 is less than unity. As from equation (24), the root λ_1 module is also less than unity, the system is stable, that is, its transients converge.

4. Partial Transients of Natural Balancing Dynamics

Let us find the general solution of the system of difference equations (5). Since eigenvalues λ_1 , λ_2 and λ_3 are different, they correspond to the eigenfunctions λ_1^k , λ_2^k and λ_3^k , where k is a number of discrete time instant. For the three eigenvectors $\Gamma_1 = \lambda_1^k (\gamma_1^{(1)} \ \gamma_2^{(1)} \ \gamma_3^{(1)})^T$, $\Gamma_2 = \lambda_2^k (\gamma_1^{(2)} \ \gamma_2^{(2)} \ \gamma_3^{(2)})^T$ and $\Gamma_3 = \lambda_3^k (\gamma_1^{(3)} \ \gamma_2^{(3)} \ \gamma_3^{(3)})^T$, one of each eigenvector coordinates can be chosen arbitrarily. Let us select $\gamma_1^{(1)} = 1$, $\gamma_1^{(2)} = 1$ and $\gamma_1^{(3)} = 1$. Then, the second and third eigenvector coordinates are found from the system of linear equations written in the matrix form:

$$\begin{pmatrix} a_{11}^{(1)} - \lambda_i & a_{12}^{(1)} & a_{13}^{(1)} \\ a_{21}^{(1)} & a_{22}^{(1)} - \lambda_i & a_{23}^{(1)} \\ a_{31}^{(1)} & a_{32}^{(1)} & a_{33}^{(1)} - \lambda_i \end{pmatrix} \begin{pmatrix} 1 \\ \gamma_2^{(i)} \\ \gamma_3^{(i)} \end{pmatrix} = 0 \quad (29)$$

The system (29) is linear dependent, so no matter which equations are used for finding $\gamma_2^{(i)}$ and $\gamma_3^{(i)}$. Substituting in equation (29) in turn λ_1 , λ_2 and λ_3 and expanding the result into a series yield

$$\gamma_2^{(1)} = -\frac{\omega L}{3}(1+r^2)\beta + \frac{r(1+r^2)(3D+1)\omega L}{9(-1+D)}\beta^2 + \dots \quad (30)$$

$$\gamma_3^{(1)} = \frac{\omega L}{3}(1+r^2)r_c\beta + \frac{r_c r(1+r^2)\omega L}{3}\beta^2 + \dots \quad (31)$$

$$\gamma_2^{(2)} = \frac{3\omega L(1+j\sqrt{r_c})}{(1+r_c)}\beta^{-1} + \frac{r\omega L\left(\frac{1}{3}(2r_c^2-11r_c-1)(3D+1)+8r_c-j\sqrt{r_c}(9Dr_c-3D-r_c+3)\right)}{(1+r_c)^2(-1+D)} + \dots \quad (32)$$

$$\gamma_3^{(2)} = \frac{3\omega L\sqrt{r_c}(\sqrt{r_c}+j)}{(1+r_c)}\beta^{-1} + \frac{r\omega L\left((1-r_c)\left(5D-\frac{7}{3}\right)-2D-\frac{2}{3}+j\sqrt{r_c}(9Dr_c-3D-5r_c-1)\right)}{(1+r_c)^2(-1+D)} + \dots \quad (33)$$

$$\gamma_2^{(3)} = \frac{3\omega L(1-j\sqrt{r_c})}{(1+r_c)}\beta^{-1} + \frac{r\omega L\left(\frac{1}{3}(2r_c^2-11r_c-1)(3D+1)+8r_c+j\sqrt{r_c}(9Dr_c-3D-r_c+3)\right)}{(1+r_c)^2(-1+D)} + \dots \quad (34)$$

$$\gamma_3^{(3)} = \frac{3\omega L\sqrt{r_c}(\sqrt{r_c}-j)}{(1+r_c)}\beta^{-1} + \frac{r\omega L\left((1-r_c)\left(5D-\frac{7}{3}\right)-2D-\frac{2}{3}-j\sqrt{r_c}(9Dr_c-3D-5r_c-1)\right)}{(1+r_c)^2(-1+D)} + \dots \quad (35)$$

The general solution of equation (5) can be written as

$$X^{(1)}(k) = Q_1\lambda_1^k \begin{pmatrix} 1 \\ \gamma_2^{(1)} \\ \gamma_3^{(1)} \end{pmatrix} + Q_2\lambda_2^k \begin{pmatrix} 1 \\ \gamma_2^{(2)} \\ \gamma_3^{(2)} \end{pmatrix} + Q_3\lambda_3^k \begin{pmatrix} 1 \\ \gamma_2^{(3)} \\ \gamma_3^{(3)} \end{pmatrix} \quad (36)$$

where Q_1 , Q_2 and Q_3 are arbitrary constants.

Using a general solution, let us find a particular solution of a homogeneous system, that is, a solution at zero supply voltage. For the initial time instant $k = 0$, let the inductor current value be i_0 , and the capacitors voltages $v1_0$ and $v2_0$. Then, equation (36) can be rewritten as

$$\begin{pmatrix} i_0 \\ v1_0 \\ v2_0 \end{pmatrix} = Q_1 \begin{pmatrix} 1 \\ \gamma_2^{(1)} \\ \gamma_3^{(1)} \end{pmatrix} + Q_2 \begin{pmatrix} 1 \\ \gamma_2^{(2)} \\ \gamma_3^{(2)} \end{pmatrix} + Q_3 \begin{pmatrix} 1 \\ \gamma_2^{(3)} \\ \gamma_3^{(3)} \end{pmatrix} \quad (37)$$

Solving the equation (37) with respect to Q_1 , Q_2 and Q_3 yields

$$Q_1 = i_0 - \frac{v1_0 + v2_0}{3\omega L} \beta + O(\beta^2) \quad (38)$$

$$Q_2 = \left(\frac{1}{6\omega L} - j \frac{\sqrt{r_c}}{6\omega L} \right) v1_0 \beta + \left(\frac{1}{6\omega L} + j \frac{1}{6\omega L \sqrt{r_c}} \right) v2_0 \beta + O(\beta^2) \quad (39)$$

$$Q_3 = \left(\frac{1}{6\omega L} + j \frac{\sqrt{r_c}}{6\omega L} \right) v1_0 \beta + \left(\frac{1}{6\omega L} - j \frac{1}{6\omega L \sqrt{r_c}} \right) v2_0 \beta + O(\beta^2) \quad (40)$$

Using equation (26) for complex roots, rewriting the eigenfunctions in trigonometric form, we have

$$\lambda_{2,3}^k = M^k (\cos(k\varphi) \mp j \cdot \sin(k\varphi)) \quad (41)$$

Substituting equations (38)–(40) into equation (37) and accounting for equation (41) yield

$$i_L(k) = F_{11} \lambda_1^k + F_{12} M^k \cos(k\varphi) + F_{13} M^k \sin(k\varphi) \quad (42)$$

$$v_{C_1}(k) = F_{21} \lambda_1^k + F_{22} M^k \cos(k\varphi) + F_{23} M^k \sin(k\varphi) \quad (43)$$

$$v_{C_2}(k) = F_{31} \lambda_1^k + F_{32} M^k \cos(k\varphi) + F_{33} M^k \sin(k\varphi) \quad (44)$$

where

$$F_{11} = i_0 - \frac{v1_0 + v2_0}{3\omega L} \beta + O(\beta^2)$$

$$F_{12} = \frac{\beta}{3\omega L} v1_0 + \frac{\beta}{3\omega L} v2_0 + O(\beta^2)$$

$$F_{13} = -\frac{\sqrt{r_c}}{3\omega L} \beta v1_0 + \frac{1}{3\omega L \sqrt{r_c}} \beta v2_0 + O(\beta^2)$$

$$F_{21} = -\frac{\omega L}{3} (1+r^2) \beta i_0 + O(\beta^2)$$

$$F_{22} = \frac{\omega L}{3} (1+r^2) \beta i_0 + v_{C_1}(0) + O(\beta^2)$$

$$F_{23} = \frac{\omega L \sqrt{r_c}}{3} (1+r^2) \beta i_0 + \frac{1}{\sqrt{r_c}} v2_0 - \frac{2r(3D+1)\beta}{9(-1+D)\sqrt{r_c}} ((r_c - 1)v1_0 + v2_0) + O(\beta^2)$$

$$F_{31} = -\frac{\omega L r_c}{3} (1+r^2) \beta i_0 + O(\beta^2)$$

$$F_{32} = \frac{\omega L r_c}{3} (1+r^2) \beta i_0 + v_2_0 + O(\beta^2)$$

$$F_{33} = -\frac{\omega L r_c (1+r^2) \beta}{3} i_0 - \sqrt{r_c} v_1_0 + \frac{2r(3D+1)\beta}{9(-1+D)\sqrt{r_c}} ((r_c-1)v_2_0 - r_c v_1_0) + O(\beta^2)$$

To obtain a particular solution of a non-homogeneous system of equations (a partial transient process, according to the terminology used in Reznikov et al. (2019), that is, for the case of a non-zero supply voltage, it is necessary to find the steady-state values of the inductor current and capacitors' voltages. These values exist because, as noted earlier, the system is stable.

First, find the vector $B^{(1)}$ using equation (4). By carrying out the operations in equation (4) and making a series expansion, vector $B^{(1)}$ is found as

$$B^{(1)} = \begin{pmatrix} \frac{2D}{\omega L(1-D)} \beta - \frac{2r(3D^2-2D+5)}{3\omega L(1-D)^2} \beta^2 + O(\beta^3) \\ -\frac{2(1+r^2)}{3(1-D)} \beta^2 + \frac{2r(1+r^2)(5-3D)}{9(1-D)^2} \beta^3 + O(\beta^4) \\ -\frac{r_c(1+r^2)(3D-1)}{3(1-D)} \beta^2 + \frac{2r_c r(1+r^2)(2-D)(1+D)}{3(1-D)^2} \beta^3 + O(\beta^4) \end{pmatrix} \quad (45)$$

The steady-state values of the vector $X^{(1)}$ coordinates are found from equation (37), for k striving to ∞ . Since the partial transient tends to 0, it is possible to equate vectors at t_{k+1} and t_k for large k . Then, after denoting the desired vector $X^{(1)(\infty)}$,

$$X^{(1)}(\infty) = A^{(1)} X^{(1)}(\infty) + B^{(1)} V / 2 \quad (46)$$

From equation (46), $X^{(1)(\infty)}$ becomes

$$X^{(1)}(\infty) = \begin{pmatrix} i_L(\infty) \\ v_{C_1}(\infty) \\ v_{C_2}(\infty) \end{pmatrix} = (E - A^{(1)})^{-1} B^{(1)} V / 2 \quad (47)$$

By calculating vector $X^{(1)(\infty)}$ and making a power series expansion, $X^{(1)(\infty)}$ is found as

$$X^{(1)}(\infty) = \begin{pmatrix} \frac{D}{R} + r \frac{3D-1}{3R} \beta + O(\beta^2) \\ \frac{2}{3} - \frac{(1+r^2)D}{6r} \beta + O(\beta^2) \\ \frac{4}{3} - \frac{r_c(1+r^2)D}{6r} \beta + O(\beta^2) \end{pmatrix} \frac{V}{2} \quad (48)$$

Using vector $X^{(1)}$ coordinates for $k = \infty$, the non-homogeneous system particular solution is obtained from equation (37) with the replacement in Q_1 , Q_2 and Q_3 initial conditions i_0 by $i_0 - i_L(\infty)$, $v1_0$ by $v1_0 - v_{C_1}(\infty)$ and $v2_0$ by $v2_0 - v_{C_2}(\infty)$ and addition of the term $X^{(1)}(\infty)$ on the right side.

An interesting specific case is making power-up for an FCC at zero initial conditions $i_0 = 0$, $v1_0 = 0$ and $v2_0 = 0$. Corresponding calculations lead to the following expressions:

$$i_L(k) = i_L(\infty) + I_1 \lambda_1^k + I_2 M^k \cos(k\varphi) + I_3 M^k \sin(k\varphi) \quad (49)$$

$$v_{C_1}(k) = v_{C_1}(\infty) + U_1 \lambda_1^k + U_2 M^k \cos(k\varphi) + U_3 M^k \sin(k\varphi) \quad (50)$$

$$v_{C_2}(k) = v_{C_2}(\infty) + U_3 \lambda_1^k + U_4 M^k \cos(k\varphi) + U_5 M^k \sin(k\varphi) \quad (51)$$

where up to small values of the first order

$$I_1 = \left(-\frac{D}{R} - \frac{r(3D-5)}{3R} \beta \right) \frac{V}{2}, \quad I_2 = -\frac{4r}{3R} \beta \frac{V}{2}, \quad I_3 = \frac{4r(r_c-2)}{9R\sqrt{r_c}} \beta \frac{V}{2}, \quad U_1 = \frac{(1+r^2)D}{6r} \beta \frac{V}{2},$$

$$U_2 = -\frac{V}{3}, \quad U_3 = \left(-\frac{4}{3\sqrt{r_c}} + \frac{4(3D+1)(1+r_c)r}{27\sqrt{r_c}(-1+D)} \beta \right) \frac{V}{2}, \quad U_4 = r_c \frac{(1+r^2)D}{6r} \beta \frac{V}{2}, \quad U_5 = -\frac{2V}{3},$$

$$U_6 = \left(-\frac{2\sqrt{r_c}}{3} - \frac{4(3D+1)r(r_c-2)}{27\sqrt{r_c}(-1+D)} \beta \right) \frac{V}{2}$$

and $i_L(\infty)$, $v_{C_1}(\infty)$ and $v_{C_2}(\infty)$ are taken from equation (48).

The found partial transient corresponds to the time interval 1 as the first one of the PWM period. Five other partial transients are calculated in a similar way using the matrices $A^{(n)}$ and vectors $B^{(n)}$ for $n = 2, 3, \dots, 6$. As mentioned earlier, these matrices and vectors differ from $A^{(1)}$ and $B^{(1)}$ by cyclic permutation of factor indices. For example, $A^{(2)} = A_1 A_6 A_5 A_4 A_3 A_2$ and $B^{(2)} = A_1(A_6(A_5(A_4(A_3 B_2 + B_3) + B_4) + B_5) + B_6) + B_1$. Owing to the lack of space, only final results for the partial transient calculation will be presented. Let us introduce the auxiliary functions:

$$s_1(m) = \begin{cases} 1, & m = 1, 2, 4, 6 \\ -1, & m = 3, 5 \end{cases}, \quad s_2(m) = \begin{cases} -1, & m = 1, 6 \\ 0, & m = 2, 3 \\ 1, & m = 4, 5 \end{cases}, \quad s_3(m) = \begin{cases} 1, & m = 1, 2, 3, 6 \\ -2, & m = 4, 5 \end{cases},$$

$$s_4(m) = \begin{cases} 1, & m = 1, 4, 5, 6 \\ -2, & m = 2, 3 \end{cases}, \quad s_5(m) = \begin{cases} 1, & m = 1, 2, 3, 6 \\ -2, & m = 4, 5 \end{cases},$$

$$\text{offs}_1(m) = \begin{cases} -\frac{5}{3}, & m = 1, 4 \\ -\frac{1}{3}, & m = 2, 3 \\ 1, & m = 5, 6 \end{cases}, \quad \text{offs}_2(m) = \begin{cases} -2, & m = 1, 6 \\ 4, & m = 2, 3 \\ 1, & m = 4, 5 \end{cases}$$

Then

$$i_L^{(n)}(k) = i_L^{(n)}(\infty) + I_1^{(n)} \lambda_1^k + M^k (I_2^{(n)} \cos(k\varphi) + I_3^{(n)} \sin(k\varphi)) \quad (52)$$

$$v_{C_1}^{(n)}(k) = v_{C_1}^{(n)}(\infty) + U_1^{(n)} \lambda_1^k + M^k (U_2^{(n)} \cos(k\varphi) + U_3^{(n)} \sin(k\varphi)) \quad (53)$$

$$v_{C_2}^{(n)}(k) = v_{C_2}^{(n)}(\infty) + U_4^{(n)} \lambda_1^k + M^k (U_5^{(n)} \cos(k\varphi) + U_6^{(n)} \sin(k\varphi)), \quad (54)$$

where up to small values of the first order

$$I_1^{(n)} = \left(-\frac{D}{R} + \frac{s_1(n)r(D + \text{offs}_1(n))}{R} \beta \right) \frac{V}{2}, \quad I_2^{(n)} = \frac{4rs_2(n)}{3R} \beta \frac{V}{2}, \quad I_3^{(n)} = \frac{4r(r_c + \text{offs}_2(n))s_3(n)}{9R\sqrt{r_c}} \beta \frac{V}{2},$$

$$U_1^{(n)} = \frac{s_4(n)(1+r^2)D}{6R} \beta \frac{V}{2}, \quad U_2^{(n)} = -\frac{V}{3}, \quad U_3^{(n)} = \left(-\frac{4}{3\sqrt{r_c}} + \frac{4(3D+1)r(r_c+1)}{27\sqrt{r_c}(-1+D)} \beta \right) \frac{V}{2},$$

$$U_4^{(n)} = \frac{s_5(n)(1+r^2)D}{6r} \beta \frac{V}{2}, \quad U_5^{(n)} = -\frac{2V}{3}, \quad U_6^{(n)} = \left(\frac{2\sqrt{r_c}}{3} - \frac{4(3D+1)r(r_c-2)}{27\sqrt{r_c}(-1+D)} \beta \right) \frac{V}{2},$$

$$i_L^{(n)}(\infty) = \left(\frac{D}{R} + \frac{(-1)^{n-1}r(D-1/3)}{R} \beta \right) \frac{V}{2},$$

$$v_{C_1}^{(n)}(\infty) = \left(\frac{2}{3} - \frac{s_4(n)(1+r^2)D}{6r} \beta \right) \frac{V}{2}, \quad v_{C_2}^{(n)}(\infty) = \left(\frac{4}{3} - \frac{s_4(n)(1+r^2)D}{6r} \beta \right) \frac{V}{2}$$

To complete the partial transients' calculation, let us continue obtained functions from discrete points of time to the entire time axis. This process involves replacement of functions λ^k by exponents with decay factor $\sigma = \ln(\lambda)/T_{PWM}$ and also replacement of trigonometric functions argument $k\varphi$ by Ωt , where $\Omega = \varphi/T_{PWM}$. Substitution of equation (24) for λ_1 and equation (27) for M followed by a power series expansion yields the following expressions:

$$\sigma_1 = \frac{1}{T_{PWM}} \left(\frac{4r}{-1+D} \beta + \frac{2r(1+r^2)(3D+1)(r_c+1)}{9(-1+D)} \beta^3 + O(\beta^4) \right) \quad (55)$$

$$\sigma_2 = \frac{1}{T_{PWM}} \left(\frac{r(1+r^2)(3D+1)(r_c+1)}{9(-1+D)} \beta^3 + O(\beta^4) \right) \quad (56)$$

5. Natural Balancing Dynamics

In accordance with the definition of the transient in the FCC given in Reznikov et al. (2019), it is necessary to find the arithmetic mean of all partial transients. Performing these simple calculations and also neglecting small values of order higher than the first lead to the following results:

$$\bar{i}_L(t) = \bar{i}_L(\infty) + \bar{I}_1 \exp(\sigma_1 t) + \exp(\sigma_2 t) (\bar{I}_2 \cos \Omega t + \bar{I}_3 \sin \Omega t) \quad (57)$$

$$\bar{v}_{C_1}(t) = \bar{v}_{C_1}(\infty) + \bar{U}_1 \exp(\sigma_1 t) + \exp(\sigma_2 t) (\bar{U}_2 \cos \Omega t + \bar{U}_3 \sin \Omega t) \quad (58)$$

$$\bar{v}_{C_2}(t) = \bar{v}_{C_2}(\infty) + \bar{U}_4 \exp(\sigma_1 t) + \exp(\sigma_2 t) (\bar{U}_5 \cos \Omega t + \bar{U}_6 \sin \Omega t) \quad (59)$$

where

$$\begin{aligned}\bar{i}_L(\infty) &= \frac{D}{2R}V, \quad \bar{I}_1 = -\frac{D}{2R}V, \quad \bar{I}_2 = 0, \quad \bar{I}_3 = 0, \\ \bar{v}_{C_1}(\infty) &= \frac{V}{3}, \quad \bar{U}_1 = 0, \quad \bar{U}_2 = -\frac{V}{3}, \quad \bar{U}_3 = \left(-\frac{2}{3\sqrt{r_c}} + \frac{2r(r_c+1)(3D+1)\beta}{27\sqrt{r_c}(-1+D)} \right) V, \\ \bar{v}_{C_2}(\infty) &= \frac{2V}{3}, \quad \bar{U}_4 = 0, \quad \bar{U}_5 = -\frac{2V}{3}, \quad \bar{U}_6 = \left(\frac{\sqrt{r_c}}{3} - \frac{2r(r_c-2)(3D+1)\beta}{27\sqrt{r_c}(-1+D)} \right) V\end{aligned}$$

Substituting instead of β, r_c, r their values yields

$$\bar{i}_L(t) = \frac{D}{2R}V(1 - \exp(\sigma_1 t)) \quad (60)$$

$$\bar{v}_{C_1}(t) = \frac{V}{3} \left(1 - \exp(\sigma_2 t) \left(\cos \Omega t - \sqrt{\frac{C_2}{C_1}} \left(2 + \frac{(C_1 + C_2)(3D+1)RT_{PWM}}{18LC_2} \right) \sin \Omega t \right) \right) \quad (61)$$

$$\bar{v}_{C_2}(t) = \frac{2V}{3} \left(1 - \exp(\sigma_2 t) \left(\cos \Omega t - \sqrt{\frac{C_1}{C_2}} \left(\frac{1}{2} + \frac{(C_1 - 2C_2)(3D+1)RT_{PWM}}{36LC_1} \right) \sin \Omega t \right) \right) \quad (62)$$

with

$$\sigma_1 = -\frac{R}{L}, \quad \sigma_2 = -\frac{RT_{PWM}^2(C_1 + C_2)}{144L^2C_1C_2}(3D+1)(1-D)^2, \quad \Omega = \frac{(1-D)^2 T_{PWM}}{8L\sqrt{C_1C_2}}$$

The found σ_1 and σ_2 values correspond to the time constants in Reznikov and Ruderman (2009) (formulas (20) and (24)).

6. Discussion

In Figures 2 and 3, simulation results are compared with theoretical ones for two sets of parameters: set 1 – $L = 0.0004$ H, $C_1 = C_2 = 0.0001$ F, $R = 1$ Ω , $T_{PWM} = 0.0001$ s, $D = 0.5$ and $V = 100$ V and set 2 – $L = 0.0006$ H, $C_1 = 0.0001$ F, $C_2 = 0.0002$ F, $R = 0.8$ Ω , $T_{PWM} = 0.0005$ s, $D = 0.8$, $V = 100$ V.

Figures 2a and 3a show the graphs of the capacitors' voltage simulation (the green curve for v_{C_1} and the light blue curve for v_{C_2}) and the transition process calculated by the formulas (61) and (62) (the black curve). Figures 2b and 3b show similar curves for the inductor current. Black curve is calculated by formula (60). Magenta curves on all the pictures correspond to simulation curves filtered by a first-order filter with a time constant T_f . These curves serve as a reference for comparison with theoretical ones. For the voltage curves, the time constant was selected as $T_f = T_{PWM}$ for the current curve – $T_f = T_{PWM}/2$. All four figures show good agreement between the simulation and calculation results.

Despite the fact that we obtained the transients of the system of third order, in practice, the inductor current transient does not differ significantly of exponent curve and the transients of the capacitors voltages does not differ of oscillating curves modulated by exponent curve, that is the second-order process. The voltage exponent decays much slowly compared with the current one because for the set 1 of selected parameters, $\sigma_1 = -2500\text{s}^{-1}$

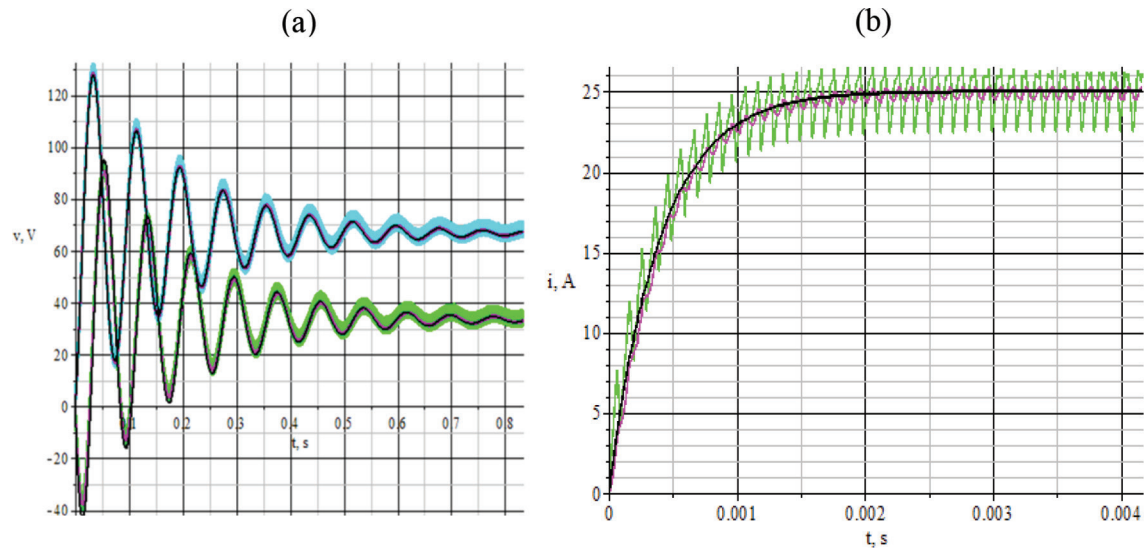


Fig. 2. The capacitors' voltage transients (a) and the inductor current transient (b) for set 1.

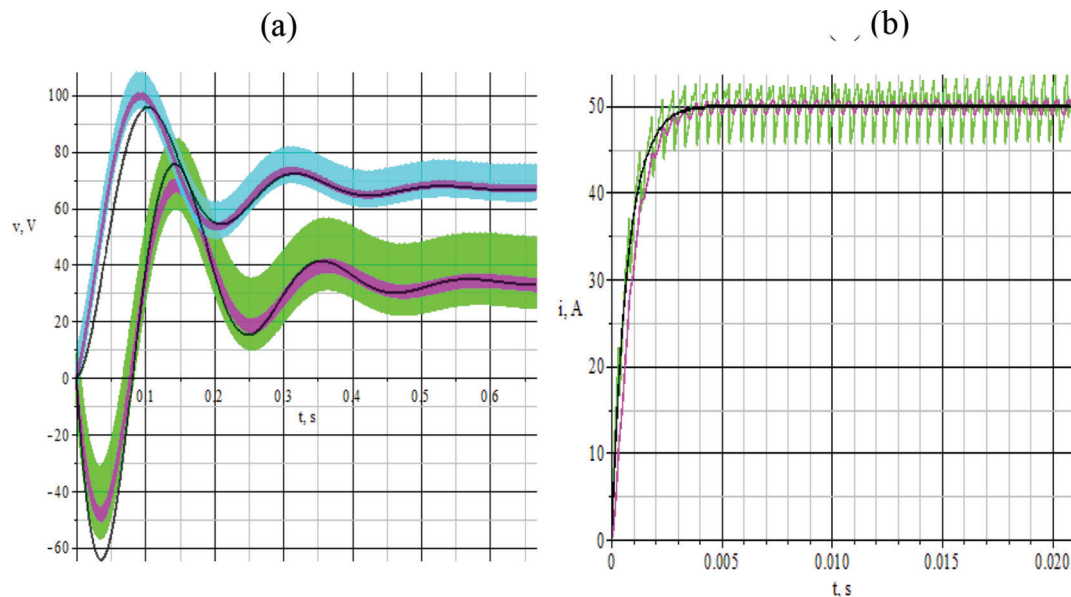


Fig. 3. The capacitors' voltage transients (a) and the inductor current transient (b) for set 2.

and $\sigma_2 = -5.425s^{-1}$ and for the set 2, $\sigma_1 = -1333s^{-1}$ and $\sigma_2 = -7.870s^{-1}$. The current steady-state value amounts to $\bar{i}_L(\infty) = VD/(2R) = 25$ A for the set 1 and $\bar{i}_L(\infty) = 50$ A for the set 2; the same is for voltages $-\bar{v}_{C_1}(\infty) = V/3 = 33$ V and $\bar{v}_{C_2}(\infty) = 2V/3 = 67$ V for the both sets.

7. Conclusion

The article presents the time domain analysis of the four-level DC–DC FCC for large values of reference voltage D . The curves corresponding to obtained formulas (60)–(62) on the graphs practically coincide with the accurate simulation ones in which oscillations in “short” time are averaged by the low-pass filter. Theoretical formulas (60)–(62) are very simple and at the same time accurately describe the “long”-time processes in the four-level FCC at large D values.

References

- Reznikov, B. and Ruderman, A. (2009). Four-Level Single-Leg Flying Capacitor Converter Voltage Balance Dynamics Analysis. In: *Proceedings of 13th European Conference on Power Electronics and Applications*, Barcelona (Spain), September 2009, pp. 1–10.
- Reznikov B., Ruderman A. and Galanina V. (2019). Analysis of Transients in a Three-Level DC-DC Flying Capacitor Converter. Time Domain Approach. *Power Electronics and Drives*, 4(39), pp. 33–45.
- Ruderman, A. and Reznikov B. (2010). Simple Time Domain Averaging Methodology for Flying Capacitor Converter Voltage Balancing Dynamics Analysis. In: *Proceedings IEEE International Symposium on Industrial Electronics*, Bari (Italy), July 2010, pp. 1064–1069.
- Wilkinson, R. H., Meynard, T. A. and Mouton, H. du Toit (2006a). Natural Balance of Multicell Converters: The General Case. *IEEE Transactions on Power Electronics*, 21(6), pp. 1658–1666.
- Wilkinson, R. H., Meynard, T. A. and Mouton, H. du Toit (2006b). Natural Balance of Multicell Converters: The Two-Cell Case. *IEEE Transactions on Power Electronics*, 21(6), pp. 1649–1657.
- Yuang, X., Stemmler, H. and Barbi, I. (2001). Self-Balancing of the Clamping Capacitor-Voltages in the Multilevel Capacitor-Clamping-Inverter Under Sub-Harmonic PWM Modulation. *IEEE Transactions on Power Electronics*, 16(2), pp. 256–263.